Engineering Structures 195 (2019) 144–158

Contents lists available at ScienceDirect

Engineering Structures

journal homepage: www.elsevier.com/locate/engstruct

Experimental and numerical study on the seismic performance of a self-centering bracing system using closed-loop dynamic (CLD) testing

Anas Salem Issa[a], M. Shahria Alam[b,*]

[a] EME 3245, School of Engineering, The University of British Columbia, Kelowna, BC V1V 1V7, Canada
[b] EME 4225, School of Engineering, The University of British Columbia, Kelowna, BC V1V 1V7, Canada

ARTICLE INFO

Keywords:
Self-centering bracing
Closed-loop dynamic (CLD) testing
Superelastic
Shape memory alloy (SMA)
Flag-shaped hysteresis
Seismic
Numerical simulation
Experimental testing

ABSTRACT

This study investigates the seismic performance of a newly developed self-centering bracing system using a novel experimental technique named as closed-loop dynamic (CLD) testing. The bracing, named piston-based self-centering (PBSC) apparatus, employs Ni-Ti superelastic shape memory alloy (SMA) bars inside a sleeve-piston assembly for its self-centering mechanism. During cyclic tension-compression loading, the SMA bars are only subjected to tension avoiding buckling and leading to flag-shaped symmetric force-deformation hysteresis. Initially, a braced frame building fitted with PBSC is seismically designed and the preliminary sizing of the brace is determined. For testing, considering the lab capability, the brace is fabricated at a reduced scale. The process of "Closed-loop dynamic testing" starts with the brace test (step 1) under strain-rate loading to characterize the numerical model parameters (step 2), which are then scaled-up as per similitude law and implemented in a finite element software, S-FRAME's PBSC brace model (step 3). Then the braced frame building is analyzed under an earthquake (step 4) and the axial force-deformation response of the brace under consideration is captured (step 5). In order to further understand and validate the actual response of the brace under earthquake type loading, the axial deformation obtained from S-FRAME is scaled-down (step 6) and used as input parameters for testing the reduced scale brace (step 7). The obtained response (step 8) is further scaled-up and used to match the S-FRAME's PBSC model for validation (step 9). Iterations from step 3 to step 9 will be required until the experimental and numerical results converge. Convergence criteria used for this validation include both the energy dissipation capacity and initial stiffness within 10% accuracy. Reasonable agreement between the numerical and experimental results is achieved in the closed-loop dynamic testing. The PBSC brace shows excellent self-centering capability under various earthquake loadings.

1. Introduction

A recent study conducted by the Insurance Bureau of Canada estimated the overall loss after a 9.0-magnitude earthquake in British Columbia at almost $75 billion and a $61 billion loss after a 7.1-magnitude earthquake in the Quebec City-Montreal-Ottawa corridor [15], which clearly reflects the vulnerability of Canadian civil infrastructure. To avoid such scenarios in Canada, it is imperative to take immediate measures. Since seismic load, in the form of ground shaking, generates one of the most devastating forces that our infrastructure can experience, designing structures against these large forces are often uneconomic. In various building and infrastructures, different structural elements and systems resist and dissipate earthquake-induced energy by means of deformations. Once permanent deformations take place, a structure becomes difficult to fix. After a major earthquake, these structures may have to be demolished and re-built acquiring huge economic losses. For example, in the Maule (Chile) Earthquake in 2010, the economic losses were estimated to be $30 billion (loss of infrastructure alone was $20.9 billion) which is equivalent to 17% of the GDP of Chile [10]. In the Christchurch (New Zealand) Earthquake in 2011, about $20 billion economic losses (equivalent to 13% of New Zealand's GDP) were estimated. The destruction was enormous, including demolition of around 70% of downtown buildings, loss of more than 50% of heritage structures, closure of the major business district for over 18 months, and outmigration of thousands of residents [11]. Such seismically damaged infrastructures become a major economic obligation.

Unfortunately, it is very expensive to build a structure to resist earthquake deformation in the elastic range of response. To solve this problem, self-centering devices can be used along with energy

* Corresponding author.
E-mail addresses: anasalem@mail.ubc.ca (A.S. Issa), shahria.alam@ubc.ca (M.S. Alam).

https://doi.org/10.1016/j.engstruct.2019.05.103
Received 17 August 2018; Received in revised form 28 May 2019; Accepted 31 May 2019

dissipating elements in a structure to resist seismic loads. This reduces deformation demand for the structural components and reduces their damages by a big margin. Such a self-centering device can be used in the form of bracing, and restraining device (e.g. in bridges against unseating, in buildings at beam-column joint) against earthquake movements. While considering a bracing system in a building there are various kinds available where Concentrically Braced Frames (CBFs) are considered as one of the most widely used bracing systems [30]. Regrettably, the traditional tension compression bracing system cannot perform well under earthquake loads. Seismic load induces cyclic tension-compression load in the braces, which can cause them to buckle during a seismic event. After the braces buckle, the deformation of the frame increases significantly and causes the beam-column joints to go into the nonlinear range. It sometimes causes irreversible damage to the structure. Furthermore, a CBF structure is much stiffer compared to the moment resisting frame counterpart. This extra stiffness attracts much more seismic load as well as floor acceleration. Excessive acceleration can cause damage to non-structural components and can also cause weakly connected non-structural components to fall on the occupants causing serious injury or fatality.

In order to resolve buckling issues, many bracing systems have been developed by researchers in the past few decades such as Buckling Restrained Bracing (BRBs) [32], CastConnex Scorpion Yielding Brace [3], Memory Alloys for New Seismic Isolation Devices (MANSIDE) project braces [9], and Self Centering Energy Dissipation Device (SCED) [34]. BRB and Scorpion Yielding Brace resist seismic force by going into nonlinear range. They exhibit fat hysteresis loops which contribute to a higher amount of damping and thus can reduce the velocity and acceleration of the system. Unfortunately, they do not have the self-centering property. Which means if there is a permanent deformation in the structure it is very difficult to push the structure back to its original position.

The other two options SCED and MANSIDE braces offer re-centering capability but their construction is complicated and for this reason, they were not widely adopted by the construction industry. Similar to the latter two options, several researchers recently conducted experimental and numerical studies, testing and validation of newly developed self-centering bracing systems including but not limited to [2,28,29,6,31,36,37,39,38,39,38]. These include the use of SMA wires and rods, friction dampers, Fiber Reinforced Polymer (FRP) rods, and other techniques. All the adopted methods were targeting enhanced seismic performance of buildings in terms of maximizing energy dissipation and/or minimizing residual drifts. All the developed systems showed good aspects in terms of self-centering, efficient energy dissipation and flag shape hysteresis response. However, in the field of self-centering bracing systems, issues related to complexity and availability of some material still presents a challenge. In this paper, an attempt is made to solve this issue by developing a self-centering bracing system that eliminates residual deformations and is relatively easy to construct.

On the other hand, in the field of structural testing, hybrid simulation has advantages over pure numerical simulation as it addresses modeling uncertainties by replacing components that are difficult to model with physical specimens. The hybrid simulation also addresses many of the limitations associated with conventional testing methods such as the shake table test (STT). For example, since only a small portion of the structure needs to be physically constructed for hybrid simulation, it is much more economical than STT. Furthermore, the size and weight restrictions present in STT are generally high. In a hybrid simulation, size is only limited by the amount of available space in the lab, and weight is only limited by the capacities of the strong floor and reaction frame. Hybrid simulation has advantages over quasi-static test (QST) as well since inertial and damping effects can be captured, and interactions between the specimen and the rest of the structural system are accounted for, which is critical for evaluating the dynamic behavior of structural systems subjected to earthquake loading [22]. Despite the long history, there remain many challenges in structural testing that are relevant to the physical components of hybrid simulation. These challenges include, but are not limited to, multi-degrees-of-freedom control; control of rotational degrees-of-freedom; testing of extremely rigid specimens; measurement of large deformation with geometric nonlinearities, etc., and lastly the high cost associated with shake table testing and hybrid simulation [23].

In this study, a simplified testing and simulation method is proposed in order to overcome the drawbacks of STT and conventional hybrid simulation approach especially when limitations in terms of time and testing facilities exist. The proposed methodology executes the steps of the conventional hybrid simulation in an off-line mode saving a huge amount of time and effort. A similar methodology has also been used by other researches in the past, where the loading input for the specimens of their interest was extracted from an accurate dynamic analysis of the entire structure [20,35,40]. In this method, displacement-based loading protocols of a structural component are generated from several dynamic simulations of a full-scale model structure in finite element environment provided that it can accurately simulate its seismic response. Then the structural component is physically tested using the extracted loading protocols and boundary conditions to determine its seismic behavior. The loading protocol could be scaled-down based on the requirements and lab limitations. Here, a 6-story building equipped with novel Piston Based Self-Centering (PBSC) system is analyzed under different ground motions. The displacement-based loading protocols are obtained, scaled down, and applied to the physical brace specimen. The experimentally generated hysteresis response is scaled up and compared again to the original response in what is called closed-loop dynamic testing. The entire testing methodology is carried out in a closed loop environment to validate its reliability. The proposed methodology holds the advantage of hybrid simulation in terms of accurate integrated experimental testing of a real specimen with a refined numerical model and the advantage of quasi-static and dynamic testing in terms of reduced time and effort needed for the investigation. The novel PBSC bracing system [13] was developed using a device commonly seen in mechanical systems, which is a cylinder-piston assembly. Using this assembly, a brace member is able to carry a large magnitude of tension and compression forces where Nickel-Titanium (Nitinol) based superelastic shape memory alloy (SMA) bars inside a sleeve-piston assembly for its self-centering mechanism are utilized. Stable and self-centering hysteresis behavior is achieved when the system is subjected to qualifying quasi-static loading. The main objectives of this study are to determine the performance of the proposed bracing system under seismic load and validate the applicability of the closed-loop dynamic testing approach. Initially, the bracing element was fabricated and then tested using the universal testing machine under qualifying quasi-static loading protocol. In this paper, the concept of closed-loop dynamic testing is described and the application of this technique on the developed system is presented. The generated hysteresis curves from closed-loop dynamic (CLD) testing for the new system are also presented and its performance is discussed. Reasonable agreement between the numerical and experimental results is achieved in the closed-loop dynamic testing.

2. Details of the PBSC system

The idea for the PBSC device is anticipated to work mainly in a Chevron/V/X configuration bracing in buildings as shown in Fig. 1. This system can be employed for new and existing both steel, concrete, and timber structures. Other applications include a single configuration as bridge restrainer, or parallel to the beam and attached to the beam and bracing which works like a shear panel device. Also, a parallel configuration attached to top and bottom flange of beams at the beam-column joints in buildings is possible [13]. The proposed system is employed using a device commonly seen in mechanical systems, which is a cylinder-piston assembly.

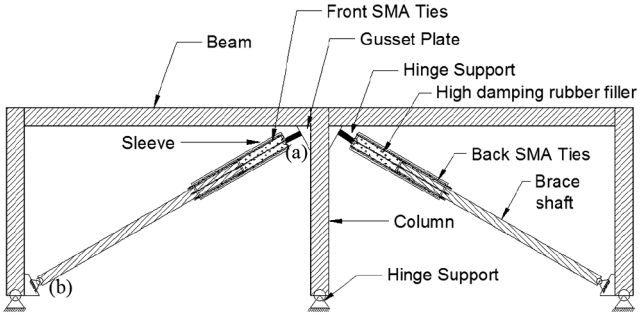

Fig. 1. Basic Components of a Piston Based Self-Centering brace.

As shown in Fig. 1, the tensile and compressive strength of a brace should be almost equal. The brace's design strength should be kept below the buckling and yield capacity of the shaft. In order to limit compression load in an individual brace, the shaft and tie arrangement shall be constructed as a piston system where the ties and part of the shaft shall be held inside a larger metal sleeve (circular, square, rectangular or any other geometric cross-section). For fabrication purposes, design drawings including the details of the PBSC arrangement are given in Fig. 2. In this system, separate ties are used to connect front plate to piston plate and back plate to piston plate. Both ends of the sleeve shall have thick metal caps to provide support for the front ties (when the system is under tension) and the back ties (while the system is under compressive load).

Two sets of ties (front and back) are connected at the shaft end plate and the other ends of the ties are connected to the cylinder/sleeve end plates using movable joints. The movable joints are constructed in such a way that they only allow the ties to go out. Inward movement of the ties will be allowed up to the ties endpoints. Locks/couplers placed at the tie ends are introduced to prevent the ties from fully entering the cylinder/sleeve. This way brace tensile and compressive loads will go through the front and back ties alternately during cyclic loading. The joint between ties and the plates also allows rotational movement without any moment generation (hinge joint). This will ensure bar straightness in the event of any kind of plate bending. The piston plate is made slightly smaller in size than the sleeve's inner dimension so that plate bending/rotation during loading does not affect the sleeve. The ties are designed for a load lower than the buckling and yield strength of the shaft and the cylinder/sleeve. When the system is under compression and the load reaches the yield load of the ties, the ties will yield and deform significantly thus lowering the axial stiffness of the system. This will, in turn, limit the axial force of the system and keep it below the buckling capacity of the shaft. In this study, the ties are made of superelastic shape memory alloy (SMA) (i.e. NiTinol) bars. Superelastic SMA bars are known for their unique property of regaining original/undeformed shape upon load removal [1,26,25]. The use of superelastic SMA bars will ensure the full self-centering capability of the brace [27]. The dimensions of the different components of the systems are shown in Fig. 2.

2.1. SMA bar machining

Two SMA rods with the diameter of 12.7 mm and length of 600 mm were used in the PBSC brace specimen. Each rod is first cut in half to have 4 SMA rods of 300 mm long each. Each of the 300 mm rods was then machined down to 8 mm diameter except for the two ends of the rods. Each end of each rod with a length of 25 mm was threaded with fine thread. The machined ends are done to install the lock nuts where they will be the support means when loading the SMA rods in tension. The steps involved in the above-mentioned machining process along with one of the machined bars are presented in Fig. 3. It is worth mentioning that high temperature can change the microstructure of the SMA and negatively affect its super-elastic response. Therefore, a cooling oil was applied to the SMA rods throughout the entire machining process in order to keep the temperature low enough so that it retains its self-centering ability.

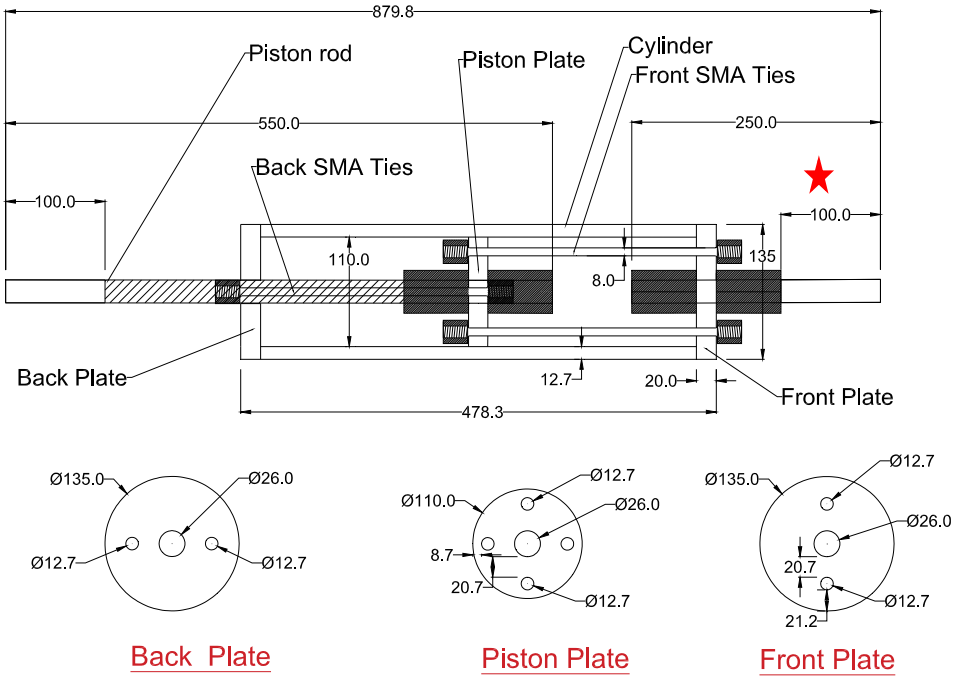

Fig. 2. PBSC brace components.

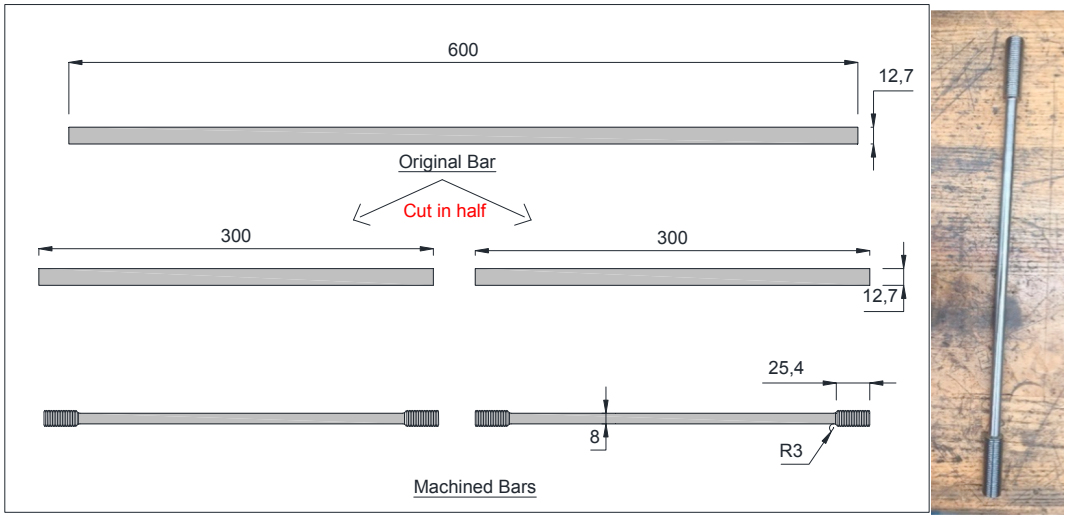

Fig. 3. SMA bar machining process.

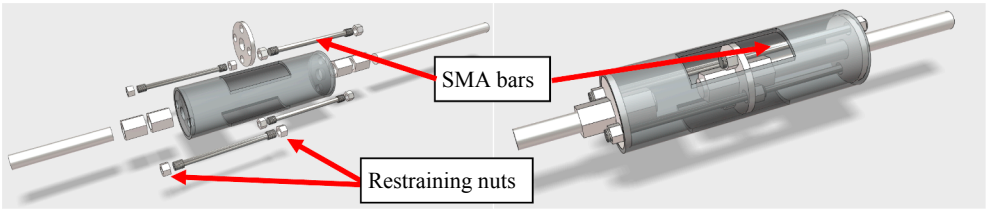

Fig. 4. Internal view of the constructed brace.

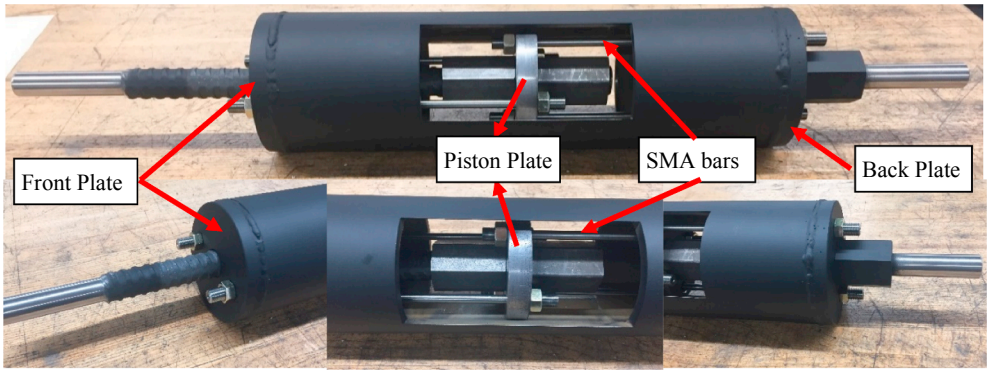

Fig. 5. PBSC brace specimen.

2.2. Specimen details

The fabrication process of the PBSC brace specimen is carried out by generating 3D models including its different components. Fig. 4 shows the internal view/arrangement of the elements. Alternatively, the structural details of the cylinder, piston and internal components, once the brace is fully constructed, are shown in Fig. 5. As shown in the latter figure, the lock nuts are installed and tightened enough to prevent the SMA rods from sliding or moving in any direction. However, this tightening was applied manually so that no significant tension force is applied to the SMA. Noteworthy, the outer body cylinder of the specimen, as well as, the supporting discs are fabricated using 12.7 mm thick steel cylinder and plates, respectively. It is critical to keep the supporting components of the system strong enough and in the elastic range as the SMA rods reach their design load capacity. Weak components, especially the outer encasing cylinder, can experience some permanent deformations which defy the entire concept of the self-centering device. The bracing system is buckling free. The SMA rods in the device are configured such that they will always experience tension regardless of whether the brace, as a whole, is under tension or compression. The nuts that are installed at both ends of each SMA rods transfer the tension load through bearing between the nut and the plates. When the brace is under tension, the front tie bars get locked with the front cap by the couplers/nuts and are under tension whereas the back tie bars are not engaged and released from loading. Under compression, i.e., when the shaft moves inside the piston, only the back ties are engaged and under tension, whereas the front ties do not experience any load. In each cycle when any of the two tie bars are under tension, the other two are released (compression-free) as they don't have nuts restraining them in the other direction. Thus, the device acts like a buckling restrained brace system.

3. Experimental investigation

3.1. Test setup

The objective of the experimental program was to investigate the seismic behavior of PBSC brace member. All the tests were carried out

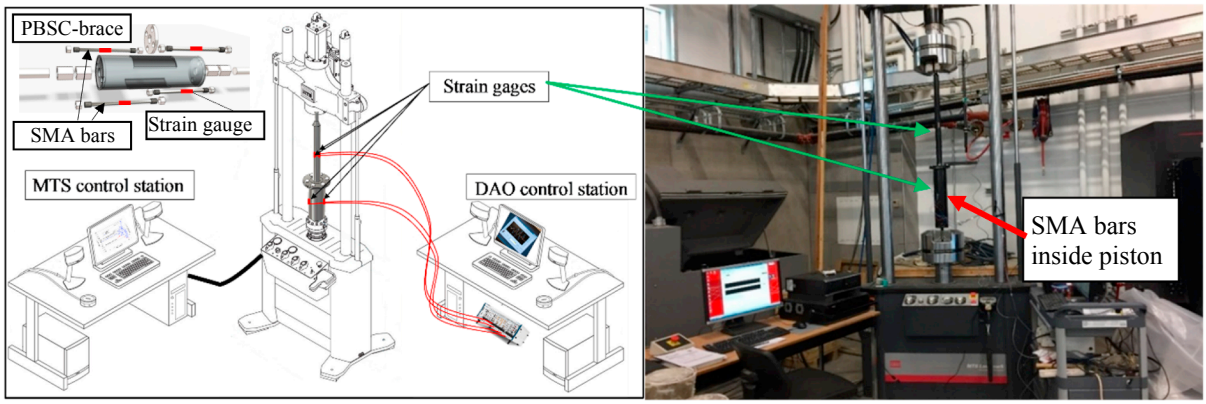

Fig. 6. Test setup.

at the Applied Laboratory for Advanced Materials and Structures (ALAMS) at the University of British Columbia (UBC)'s Okanagan campus. First, the quasi-static cyclic test was performed. The specimen was tested using the MTS universal testing machine with a capacity of 500 kN. Taking into consideration the machine dimensional limits and characteristics, together with ease of specimen handling, the experimental set-up described in Fig. 6 was adopted.

The MTS control system and the data acquisition system were both connected to the specimen to measure the different test parameters. The MTS machine is equipped with a load cell to measure the axial force as well as vertical movement transducers to measure the movement of the MTS head. Additionally, four SMA strain gauges in total were attached to the four SMA rods (as shown in Fig. 6) to get more insights into the stress-strain behavior of the SMA bars.

3.2. Loading protocol

Fig. 7 depicts the cyclic loading time history used for the PBSC brace specimen. This time history with a maximum value of 15 mm was associated with the moving head of the universal testing machine. A maximum value of 15 mm is considered so that the maximum strain in the SMA rod does not exceed its superelastic strain range of 6%. This type of Nickel-Titanium base SMA rod experiences some residual deformation after exceeding this threshold. The following loading protocol was employed by Haque and Alam [14] to numerically validate the PBSC brace; the acquired numerical simulation results are presented and compared in the following section.

4. Test results

Employing the above test setup and the loading protocol, the cyclic test was conducted. Stable and symmetric self-centering hysteresis loops were obtained as shown in Fig. 8(b). The PBSC brace showed negligible permanent deformation throughout the entire testing procedure. As mentioned previously, the permanent deformation can be avoided by applying deformations that do not exceed the SMA superelastic threshold. Therefore, a design engineer should consider such criteria when designing this bracing system. The SMA bar lengths should be selected based on the expected maximum deformation that the brace will experience during the design seismic event. Fig. 8(a) depicts a stress-strain plot obtained for one of the SMA rod specimen obtained from the right top bar in the device. Marginal residual deformation was observed in the test result, which could lead to sliding in the PBSC brace. However, it does not have a significant impact on the overall performance of the brace element. Additionally, the test results were compared with the numerical ones obtained by Haque and Alam [14], which are also comparable to results presented by Ozbulut [26,25] and DesRoches et al. [7]. A tension only uniaxial mechanical SE SMA material model was developed in MATLAB with residual deformation simulation capability based on the experimental stress-strain response. Next, it was utilized in a custom-built MATLAB finite element solver developed for the PBSC bracing system. Quasi-static input loading history was applied, and the resultant hysteresis was found to exhibit sliding behavior. The availability of such a tool will ease the implementation of the developed system in real life applications. The development of the numerical model in MATLAB environment is conducted in another research in which the detailed procedure can be found in Haque [12]. The hysteresis response generated in MATLAB was compared with the experimental results. The results show that the MATLAB generated axial force-deformation response was reasonable but not highly accurate in predicting the behaviour of PBSC brace just based on SMA's strain-strain response. Hence, the axial force-deformation hysteresis response of PBSC obtained from the experiment was further analyzed, and a novel flag-shaped hysteresis rule with sliding response was further developed in MATLAB and implemented in S-FRAME – a commercially available analysis and design software [12]. The stress-strain response of SMA rebar and the axial load-deformation hysteresis response of PBSC brace are presented in Fig. 8a and b, respectively. The implemented hysteresis model in S-FRAME is plotted along with the experimental results in Fig. 9, which shows very good agreement in terms of energy dissipation capacity initial and post-elastic stiffness (within 10% accuracy). The details of the implemented model are presented later in Section 5.

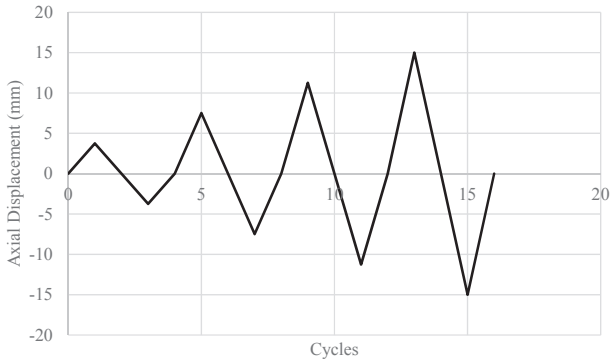

Fig. 7. Quasi-static deformation loading protocol.

4.1. Strain rate effect

To investigate the effect of different loading rates on the proposed PBSC bracing system, four higher loading rates are considered and compared to the initial rate used in the qualifying quasi-static test. Two, five, ten, and fifty times the initially used rate (i.e. 1in/

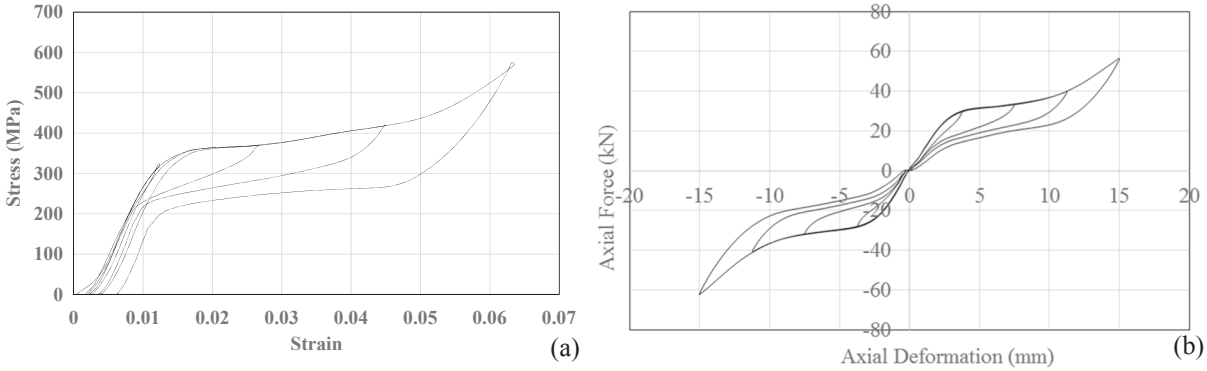

Fig. 8. (a) Stress-Strain response of a single 8 mm diameter SMA bar, (b) Hysteretic response of the PBSC bracing system.

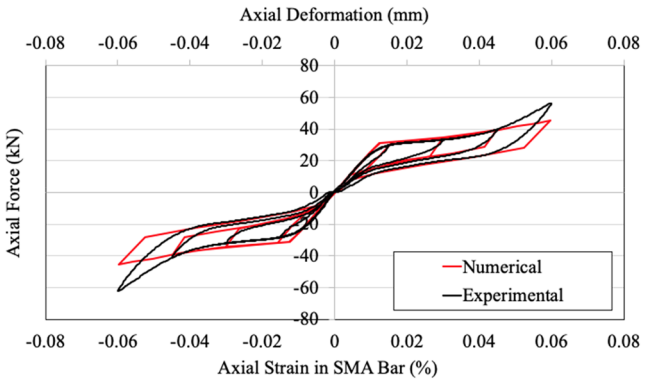

Fig. 9. Axial force versus deformation /SMA strain test results plotted with S-FRAME hysteresis model for the PBSC brace specimen.

min = 0.42 mm/s) are defined and the test is carried out on the same specimen as shown in Fig. 10. The hysteresis behavior generated for the four increasing rates are comparable (Fig. 10). As mentioned previously, the test was conducted consecutively on the same specimen without any parts replacement or maintenance. The maximum obtained force-deformation responses for the varying rates are in the range of 3% higher than the original rate (see Fig. 11). Although the maximum force-deformation responses are very close, the energy dissipation decreased noticeably as the rate increased. The maximum reduction observed for the X50 rate with around 60% less energy dissipation, as shown in Fig. 11(d). The smaller hysteresis loops can be seen in Fig. 10. As strain rate increases, the heat-exchange condition increasingly digresses from the isothermal one. The latent heat of transformation causes the SMA to heat up and then increase its average temperature during the test. At the same time, during each loading cycle, the specimen temperature oscillates around an average value, according to the variation of strain, the instantaneous temperature rises upon unloading, the forward transformation being exothermic, and decreases upon unloading, the inverse transformation being endothermic. Both the hardening of the transformation branches and the narrowing of the cycle, resulting in a reduction of energy loss, are caused by the instantaneous temperature variation. The possible increase in the average temperature produces an upward translation of the cycle [19]. It is worth mentioning that the observed change in the hysteresis behavior could also be attributed to the repeated cyclic loading since all the tests are conducted on the same specimen as concluded by DesRoches et al. [7] as well. This represents one limitation in this study and is recommended to be investigated in the future studies to use different specimens for each loading cycle.

5. Closed-loop dynamic testing

In the context of scaled-down experiments, scale effects include all response distortions that occur when one or more of the basic dimensional quantities in the FLT9 (Force-Length-Time-Temperature) system are scaled in an experiment. In earthquake engineering research, scale effects occur in quasi-static and pseudo-dynamic experiments, in which time is scaled, and in reduced-scale model experiments where the length is scaled and, as a consequence, force and time have to be scaled as well. In dynamic model tests, the scaling laws for force, time, and other dependent dimensional quantities can be derived through dimensional analysis [21]. Table A.1 (in Appendix A) summarizes scaling laws for three types of models that may be suitable for seismic response studies involving inelastic material behavior. The quantity l_r denotes the ratio of model-to-prototype length [18]. In this study, a scale of four is adopted where the length and diameter of the SMA rods is ¼ of the real brace element in the building model.

Rate	Value (mm/s)
X1	0.42
X2	0.85
X5	2.12
X10	4.23
X50	21.12

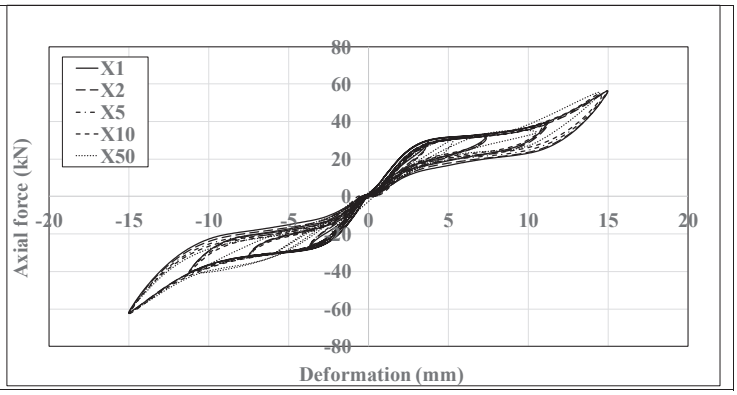

Fig. 10. Loading rate effect comparison of five different rates in PBSC.

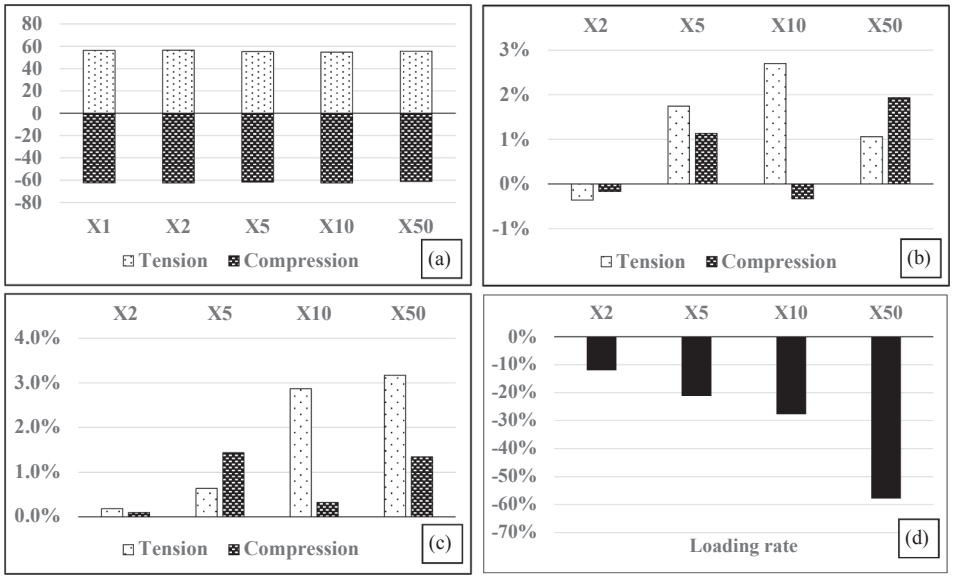

Fig. 11. Strain rate results comparisons: (a) Axial force (kN), (b) Axial force magnitude percentage variation, (c) Axial deformation percentage variation, and (d) Energy dissipation comparisons.

5.1. Closed-loop dynamic (CLD) testing concept

The concept of closed-loop dynamic testing is proposed to validate its feasibility of conducting comprehensive dynamic testing on members without the need to conduct the braced frame testing under quasi-static test or using hybrid simulation. Hybrid simulation is a testing method for observing the seismic response of structures using a hybrid model included of both physical and numerical substructures. Because of the unique feature of the method to combine physical testing with numerical simulations, it provides an opportunity to investigate the seismic response of structures in an efficient and economically feasible manner. The closed-loop dynamic testing, however, reduces the time and effort furthermore compared to conventional quasi-static testing of braced frame and hybrid simulation. In this section, the concept and the validation of this new concept are presented.

The flowchart diagram presented in Fig. 12 represents the concept adopted in this study for the proposed closed-loop dynamic (CLD) testing approach. The concept involves nine main steps: (1) Generate design drawings and fabricate a small scale specimen then test it under qualifying quasi-static loading protocol; (2) Conduct a series of experimental tests using varying loading rates to study the strain rate effect on the system; (3) Implement the hysteresis behavior obtained from experimental testing in a finite element environment and design building equipped with the PBSC; (4) Apply the dynamic load on a frame building equipped with the PBSC system; (5) Generate and extract the force-deformation hysteresis response of the brace element of interest; (6) Extract the brace deformation response as a function of time; (7) Scale down the deformation response, using the similitude laws, and apply it to the scaled-down brace specimen; (8) Extract the force-deformation hysteresis response from the test program; and (9) Scale-up, using the similitude laws, the deformation response and match it with the original response obtained from the dynamic simulation of the frame building in step (5). In details, step (9) looks at a match between the scaled experimental results and the response from the model. The convergence is checked by targeting the initial stiffness and energy dissipation (within 10%) based on the experimental results obtained from step (7). In the case of non-convergence, the input parameters are updated in the FE model from step (7) into step (3) for re-running the model. The new results obtained from step (5) are then compared to those from step (8), presented in step (9). This iterative step can be done twice or more until an acceptable matching is achieved in the margin of 10%. Further iterations might be required to meet the convergence criteria. It is a refinement procedure to achieve better matching of the results in the closed-loop dynamic testing, which is considered as a refined model after adjusting the parameters. By conducting the above-mentioned steps, the system response is studied and validated from start to finish in a closed loop as shown in Fig. 12. The above-mentioned procedures are implemented using five of the previously presented twenty earthquake ground motions and applied consecutively on the brace specimen. The details of the applied deformation-based loading protocols and the obtained results are presented in the following section.

One of the important aspects that closed-loop dynamic testing can offer is the validation of a new structural system in seismic regions. This is especially true when a recently proposed system or device is going to be employed in a structure. The closed-loop dynamic testing approach can provide a cost-effective solution in a timely manner for a new system. In this approach, the designer can fabricate the new structural component, test it under various strain rate to understand its dynamic response and validate the results numerically. Having an experimentally verified model will help the design engineer design a structure equipped with this new system and reassess the design using the closed-loop dynamic testing. For different seismic design parameters and zones, representative earthquake records can be used to perform the dynamic response validation process. A key point in this process is to perform a series of strain rate tests on the specimen in order to verify the applicability of using this technique for dynamic response verification.

5.2. Analysis model

A six-storied 4 × 4 bay steel braced frame building was considered in this study. The selected 6-story building represents a typical residential/office steel building in the city of Vancouver, and it is very common to use bracings as the lateral force resisting system in such buildings [33]. The bay widths are 5 m and story heights are 3 m each. Therefore, the total width of the building in two orthogonal directions is 20 m, and the total height is 18 m. The braces are only installed on the perimeter frames of the building as shown in Fig. 13. To design the braces for full lateral-load arising from the seismic events, all beams were connected to the columns using moment released connections; and the columns were restrained to the foundation using hinges. Nevertheless, the columns were modeled as continuous members along with their heights. The modeling was done in a way that the structure

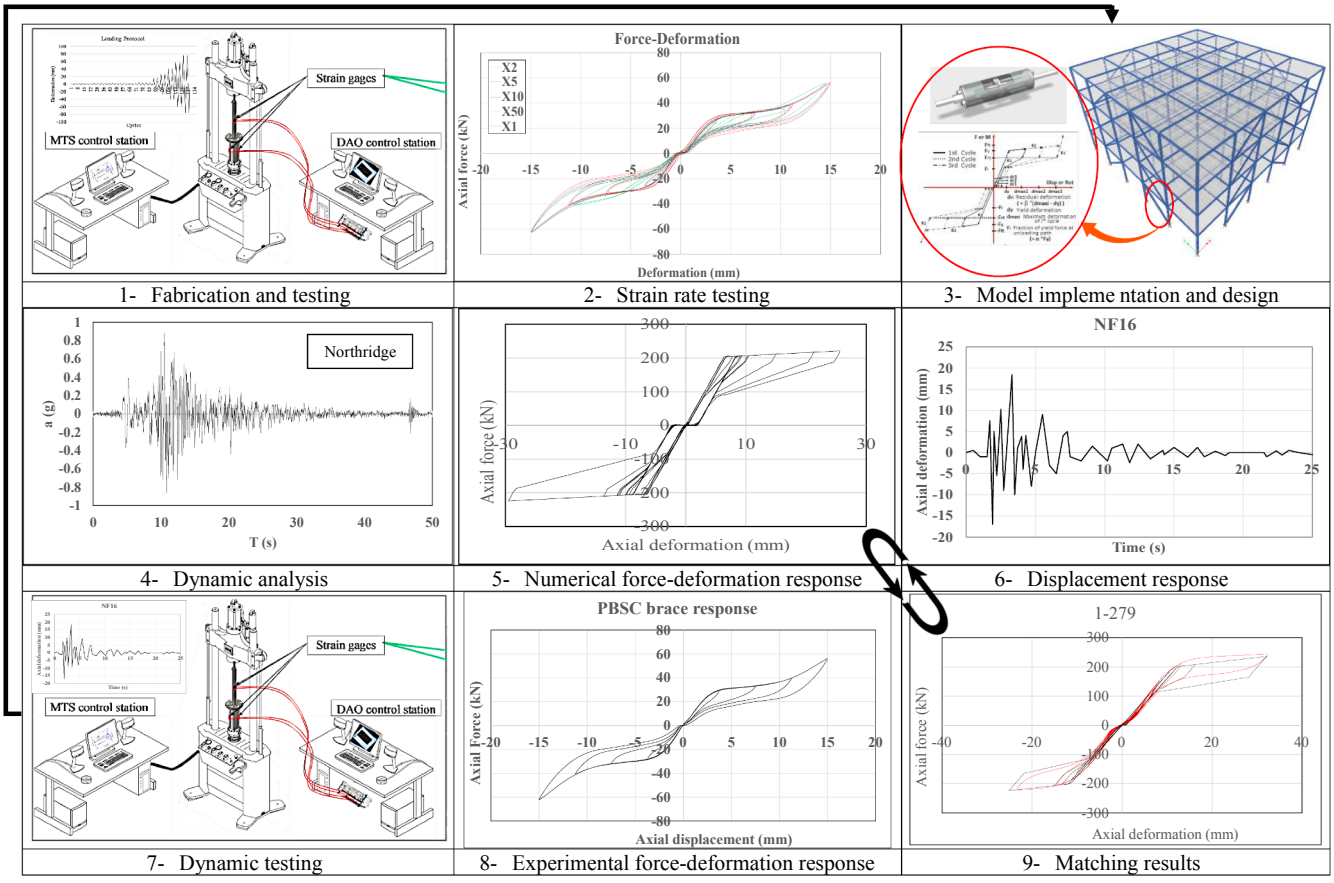

Fig. 12. Closed-loop dynamic testing flow chart procedures.

becomes unstable under lateral loading if braces are not installed. The braces were modeled using pin ended connections and were installed as inverted "V" in the middle two bays. In this configuration, only the braces will resist the lateral load arising from the earthquake. The slabs were modeled using 150 mm deep concrete shell sections. However, for clarity, it is hidden from the view in Fig. 14. The following loading values were applied to the floor slabs (except the roof) in the gravity direction. Superimposed dead load is 2 kN/m^2, and the live load is 2.4 kN/m^2. On the roof, the dead load was considered as 0.5 kN/m^2, and the snow load was taken as 2.2 kN/m^2. Furthermore, another 1.6 kN/m^2 on the roof was considered for miscellaneous storage and mechanical service loads. After the structural modeling, the frame was analyzed under both gravity and seismic loading. The seismic zone considered for this analysis was "Vancouver," and the soil class was taken as class "C." (see Table 1)

Preliminary analysis suggested the ductility-related force modification factor (R_d) and overstrength-related force modification factor (R_o) values of 6.0 and 1.1, respectively. These values were later confirmed using detailed analysis where the details can be found in [12]. The mentioned reference conducted the design and analysis of three PBSC braced frame models created in S-FRAME structural analysis and design software. These building frames were designed using [24] building code and [4] design standard. These buildings were designed using arbitrary values of R_d = 6.0 and R_o = 1.1. After the design,

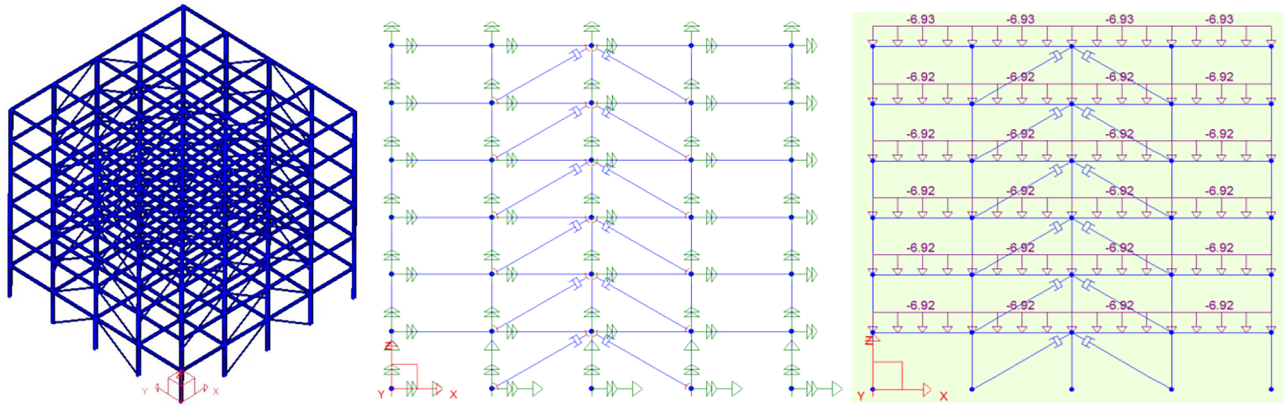

Fig. 13. Three-dimensional model of the steel building, Nodal Restraint Conditions, and Uniformly distributed gravity loading on the beam for the 2D model (from left to right).

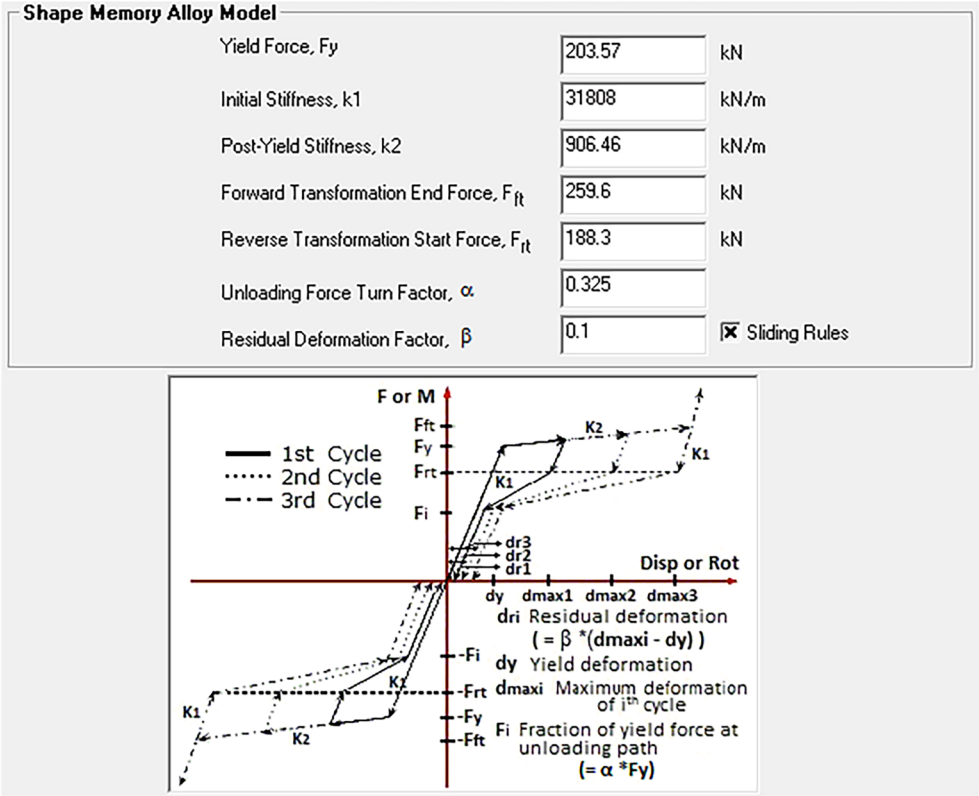

Fig. 14. Sample input data for PBSC link hysteresis.

Table 1
Spectral acceleration values for Vancouver Soil Class "C".

Sa(T)	Sa(0.2)	Sa(0.5)	Sa(1.0)	Sa(2.0)	Sa(4.0)
Acceleration (g)	0.95	0.65	0.34	0.17	0.085

nonlinear archetypes were built using hysteresis model developed for the PBSC bracing system. Finally, incremental dynamic time history analyses were carried out on the nonlinear archetypes using 44 far-field ground motion records which were normalized with respect to the record set's median PGV. From this analysis, the median collapse earthquake intensities were calculated, and they were used to calculate the collapse margin ratios. These collapse margin ratios were adjusted for spectral shape factor and finally compared against acceptable limits. It was found out that all individual archetypes and the group passed the acceptable limit of collapse margin ratios. Therefore, the initial seismic performance factor values ($R_d = 6.0$ and $R_o = 1.1$) are considered adequate for the seismic design of this system. Furthermore, designing this braced frame with a low R_d value (4 or below), may not induce nonlinearity in the braces; which will prevent utilizing the self-centering capability of this bracing system. Furthermore, if this building can resist seismic load and can also self-center after designing with a large R_d value (6.0), then the performance advantage of this novel bracing system will be confirmed. After carrying out the analysis and design using [5], it was found that the minimum required sections for the beams and columns are W250 × 24 and W310 × 67, respectively. It was also found that the minimum required sizes for the brace for the upper three floors, for the 2nd and 3rd floor, and on the ground floor is HS127 × 4.8, HS127 × 6.4, and HS127 × 8.0, respectively.

The dashpot shapes shown at the end of the braces represent the zero-length link elements. To calculate the hysteresis model's input parameters, three different PBSC braces were designed for the three different brace sections used in this frame. In order to design the PBSC braces, the ultimate design loads which were used to design the brace sections were retrieved from the S-FRAME Software. The envelopes of all the design load cases were taken and the PBSC brace was designed for it. The amount of required SMA needed for each brace was calculated using a spreadsheet specifically developed for this task. The PBSC brace design process used in the spreadsheet is as follows: the ultimate design load was divided using the austenite to martensite starting stress (σams) of SMA to find out the required cross-sectional area of SMA bars. It is worth mentioning that large diameter Nitinol is commercially available up to 32 mm and the authors have already procured them from ATI Wah Chang. Previously, authors have tested 20.6 mm diameter SMA bars under cyclic tension. For this study, the value of σams was taken as 400 MPa. The result gave the necessary cross-sectional area of the SMA bars. Bar diameters were selected in a way to provide an integer value or as close to that as possible. In the next step, a design length of the SMA bars was chosen. The estimated length of the SMA bars was taken as 1/6th of the brace length or approximately 1 m. This ratio has been selected based on the following assumption: buildings are generally designed for a maximum interstory drift of 2–2.5%. As braces are diagonal members, they typically experience 40–50% of this drift in their axial direction; which results in a drift of approximately 1%. As NiTinol based SMAs can recover from 6% to 9% strain [8], we can comfortably make the NiTinol bars of the PBSC brace 1/6th to 1/9th of the total brace length. This will also result in a reduced amount of material and cost savings. The parameters mentioned above were provided as input to the MATLAB quasi-static analyzer developed for the PBSC brace, and a hysteresis model was generated. The hysteresis results were used to find out the initial and post-yield stiffness as well as the SMA unloading stiffness. These values were provided as input parameters in the S-FRAME Software link hysteresis input window. This process was repeated three times for the three brace sections, and three links were generated. Finally, these links were assigned to the appropriate brace ends. Fig. 15 shows the link input parameters used for the

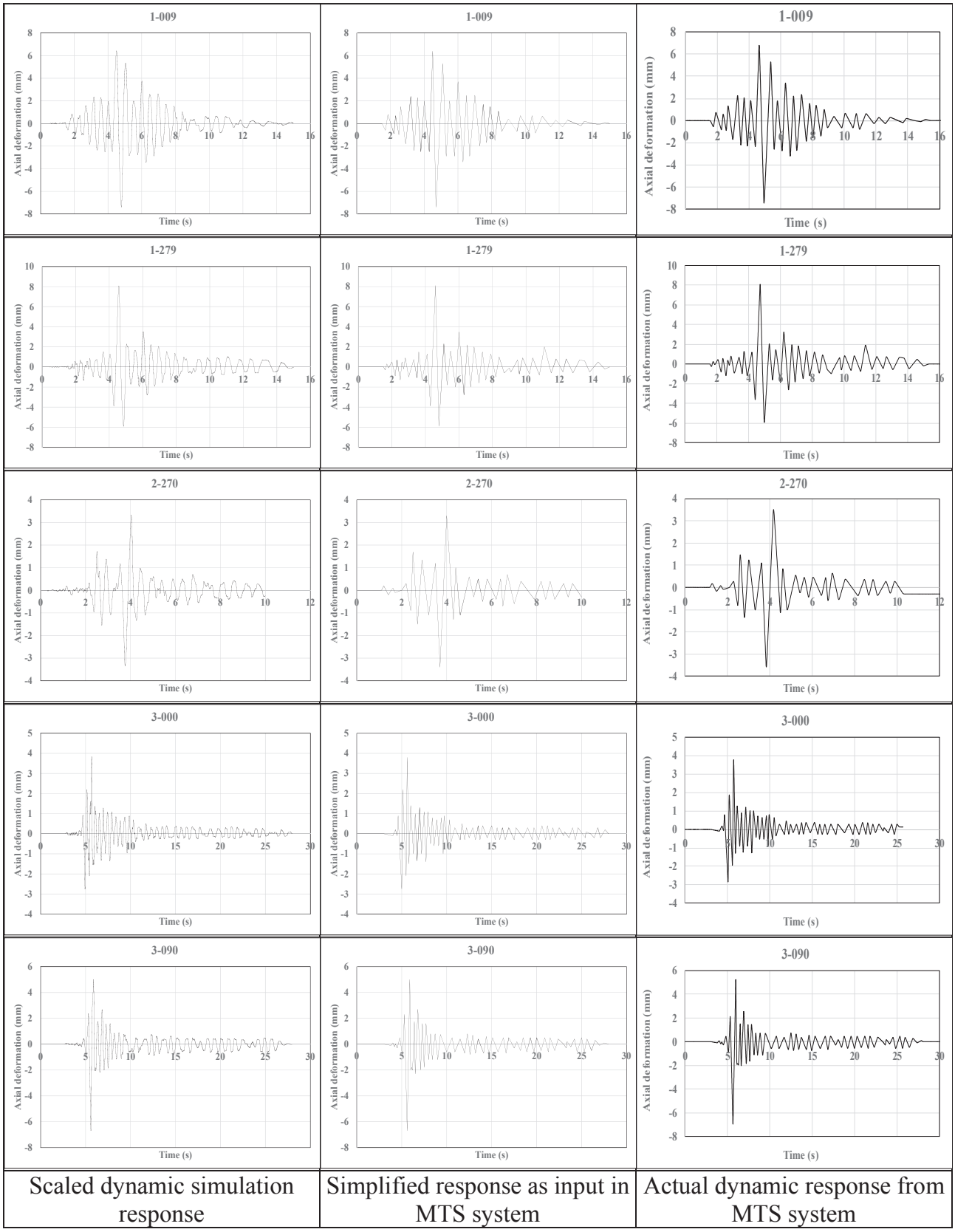

Fig. 15. Deformation dynamic response from 5 real earthquake motions.

HS127 × 8 brace section. In the studied building [12], for a bay length, L = 5000 mm and floor height, H = 3000 mm, the brace length is 5830.95 mm and the maximum considered design inter-story drift ratio, Δ/H was 0.025 or 2.5%. For a 2.5% design story drift, the axial elongation of the brace will be 0.025 * 3000 * (5/5.830) = 64 mm. The brace was designed such that the axial stiffness of the SMA part was much smaller compared to the other part of the brace so that all the axial deformation mainly concentrates in the SMA bars. In the above sentence, considering the total length of the brace (5830 mm), its axial elongation was 64/5830 = 1.1%, which mainly corresponds to SMA strain where SMA bar has 1000 mm length. Hence, SMA strain at 2.5% story drift will be 64/1000 = 0.064 = 6.4%.

It should be noted that the 2.5% design drift was considered to design a single brace element to ensure it goes beyond superelastic strain range but does not exceed its superelastic strain limit. The building was equipped with four SMA braces in each floor. Besides, it should be noted that the structural elements are always chosen larger than the required sizes during the design process to ensure capacity protected elements. This will result in a much stiffer system and reduced interstory drift. It should be also noted that the design level earthquake should not cause a structure to reach its ultimate limit state. Usually, this can be achieved through incremental dynamic analysis by linearly ramping up the earthquake records [17].

As the stress in NiTinol bars goes beyond the superelastic strain range, its stress level increases drastically. Hence, it can be safely assumed that the PBSC brace to steel frame connections need not be designed for any force generated beyond this point. Therefore, the connections between the brace and the frame will start failing after this stress in the SMA bars. Here, the built specimen represents the ¼ scale of the full-scale brace which is designed using 1000 mm long Nitinol bars. Based on that, the scaled-down bar length was 250 mm in the PBSC brace specimen.

5.3. Force-deformation hysteresis response

The highest base shear is mainly observed in the lowest story next to the ground level where braces will experience the highest force-deformation demand. A bracing element located in the first story is, therefore, considered to conduct the closed-loop dynamic testing. Five random earthquake records obtained from the Pacific Earthquake Engineering Research Center (PEER) Next-Generation Attenuation (NGA) database and matched with the UHS of Vancouver, are selected where they had different deformation response on the brace element. Some of these deformations have a high-frequency response and some with low frequency. Having different deformation frequency responses will help characterize the dynamic behavior of the brace specimen and study the strain rate effect under dynamic loading on the system.

Once the deformation responses have been obtained, they were scaled down based on the scaling factor of ¼. According to scaling laws shown in Table A.1, the deformations were divided by 4 and the time was divided by two (i.e. √1/4 = 1/2). The next step is to simplify the response into segments that can be input into the MTS control system. The different loading rates for each segment, based on the deformation and time, is also calculated and incorporated into the protocol to closely simulate the dynamic effect. As shown in Fig. 15, the accurate representation of the real response was achieved by transforming every deformation response precisely. It is worth mentioning, once the protocols have been defined, the tests are conducted successively on the specimen without altering anything, or tightening of the bolts, or with any form of maintenance.

The force-deformation responses of the five dynamic responses are obtained from the MTS control system, scaled up and compared to the original brace response in the frame building. As shown in Fig. 16, a reasonable agreement between the experimental and numerical responses is achieved. The findings support the concept of the closed-loop dynamic testing presented herein. With reduced time and effort, good results can be achieved when adopting this proposed methodology. One source of the slight variation of the results can be attributed to the simplification of the dynamic deformation response obtained from the numerical simulation and scaling up and down the results which could amplify these variations. The shown results, however, show some discrepancies in terms of maximum force, deformation, sliding effect, and overall hysteresis flag shape. The module available in S-FRAME software was developed based on finite element modeling solely. The results obtained from the experimental work is used to adjust the different values including yield force, initial stiffness, post-yield stiffness, forward transformation end force, reverse transformation start force, unloading force turn factor, residual deformation factor and sliding rules application as shown in Fig. 14.

5.4. Model modification and refinement

Based on the obtained experimental results, the numerical module in S-FRAME is modified and the dynamic analyses are re-conducted. Due to the discrepancy is the simplification of the stress-strain curve of the Nitinol which does not capture the nuances of the response, several trials were conducted by adjusting the model parameters in order to achieve more comparable results. The refined results are obtained, compared and presented in Fig. 17 where much better agreement is achieved. The results presented in Fig. 17 highlights the feasibility of the proposed closed-loop dynamic testing approach. However, care should be practiced when adopting this technique. In the PBSC presented in this study, as explained earlier, the system showed a comparable hysteresis response in various strain rates, i.e. from the original rate to all the way to X50. This facilitated the validation of the closed-loop dynamic testing concept. In systems where strain rate effect is highly noticeable and observed, the closed-loop dynamic testing can provide a similar validation like the one presented herein if the model can accurately capture the strain rate effect. Similar results were achieved on a different bracing system which can be found in Issa and Alam [16]. Further experimental investigation can be implemented on different systems to generalize the concept. Nevertheless, for systems with behavior similar to PBSC, this technique can be an affordable option to validate the design process and the feasibility of adopting new systems.

Dynamic testing of the proposed system, through closed-loop dynamic testing, highlighted the need to adjust the modeling parameters which were initially developed based on pure finite element simulation [13,14]. The adjusted parameters, based on the dynamic testing results, improved to a great extent the ability of the numerical model to capture the actual response of the system. Table 2 highlights the parameters used for capturing the system behaviour before and after refinement. Although the initial stiffness from the quasi-static cyclic test was higher than the dynamic stiffness, the global response of the FEM model with the refined parameters (‘after’ in Table 2) shows an acceptable level of average maximum inter-story drift, which was less than 0.5%. This limit is prescribed under immediate occupancy by FEMA 365 (Table C1-3) for braced steel frames. Although the PBSC bracing system is more flexible compared to traditional or buckling restrained bracing system, the stiffness of the PBSC bracing system and the structure as a whole could be adjusted by changing the length, the number, and diameter of the SMA bars. Besides, Fe-based SMA bars (with higher elastic stiffness) could be used instead of NiTinol bars, which will further increase the stiffness of the bracing and the system.

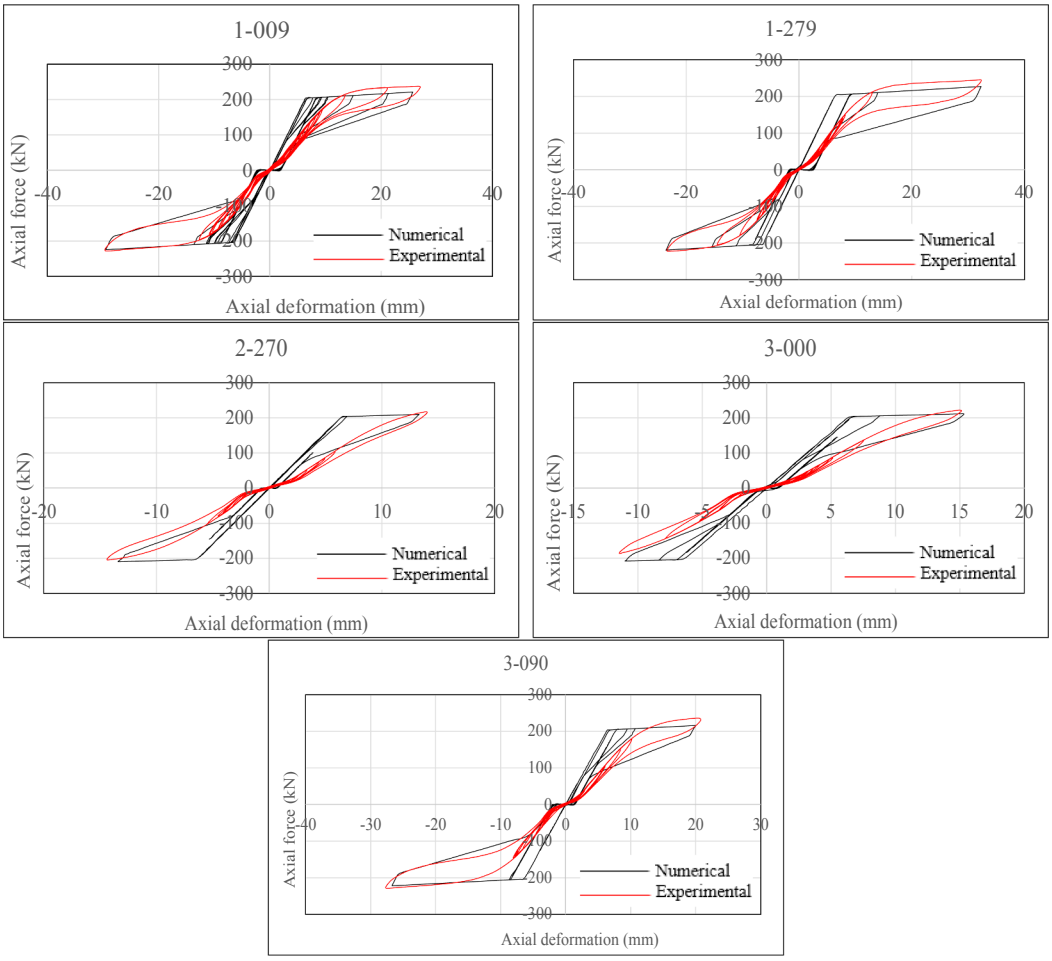

Fig. 16. Experimental and numerical hysteresis response for the 5 records using the closed-loop dynamic testing.

It should be noted that the initial parameters were obtained from the quasi-static cyclic loading test based on which the numerical brace model was calibrated. After designing the braced frame in the finite element software, seismic simulations were performed where the loading history was obtained from the deformation time history of the brace element. While testing the brace element under seismic loading, the stiffness of the brace element reduced compared to the quasi-static loading, which could be due to the slippage of SMA bars inside the threaded couplers, slippage of the back bar through the nut connected to the back plate, high strain rate effect of SMA, and/or effect of repeated cycling of SMA bars. Besides, the post-yield stiffness of SMA bar increased during the seismic loading, which is again due to the strain rate effect of SMA bar. It should be pointed out that the same SMA brace element had to be used to perform quasi-static cyclic and dynamic loading tests to understand the effect of seismic loading. The results are only valid for that brace element. Hence, the length of the SMA bar was kept the same for the test loadings where only the numerical model parameters had to be updated based on the new results.

Fig. 18(a) and (b) illustrate the comparison between the maximum and residual interstory drift ratios for the ten earthquake records with the code limit. It can be seen that the maximum interstory drift ratios for all ten earthquake records are very close to one another except the Trinidad earthquake. It can be observed that the maximum interstory drift ratios were mostly in the 3 m and 12 m level, which are the 1st and 4th floor of the building, respectively.

The maximum interstory drift value is 0.59% which is around 1/4th of the code specified limit of 2.5% for the “Other Building” category. Furthermore, the average value was found to be around 0.4% only. The residual interstory drift values varied insignificantly among the earthquake records in which the range was from almost zero to 0.02%. Like the previous plot, the maximum values are mostly observed at 3 m and 12 m level (First floor and fourth floor, respectively). The average of the maximum was around 0.005%. This value is much lower than the traditional BRB frames which experience an average 0.3% residual interstory drift ratio [41].

6. Conclusions

This paper described the development and seismic performance assessment of a novel Piston Based Self-Centering (PBSC) bracing system for the civil engineering structures. Design drawings were generated, and a test specimen was fabricated and tested several times under quasi-static loading protocol where stable and self-centering hysteresis behavior was achieved. The generated hysteresis curves for the new system were presented and its performance was discussed. This paper also described a new testing and simulation technique in order to reduce the computational and experimental requirements and efforts in structural experimentation and validation. In this approach, displacement-based protocols generated from dynamic simulations of a 6-story building equipped with PBSC system were obtained, scaled down, and applied for the fabricated brace specimen. The experimentally generated hysteresis responses were scaled up

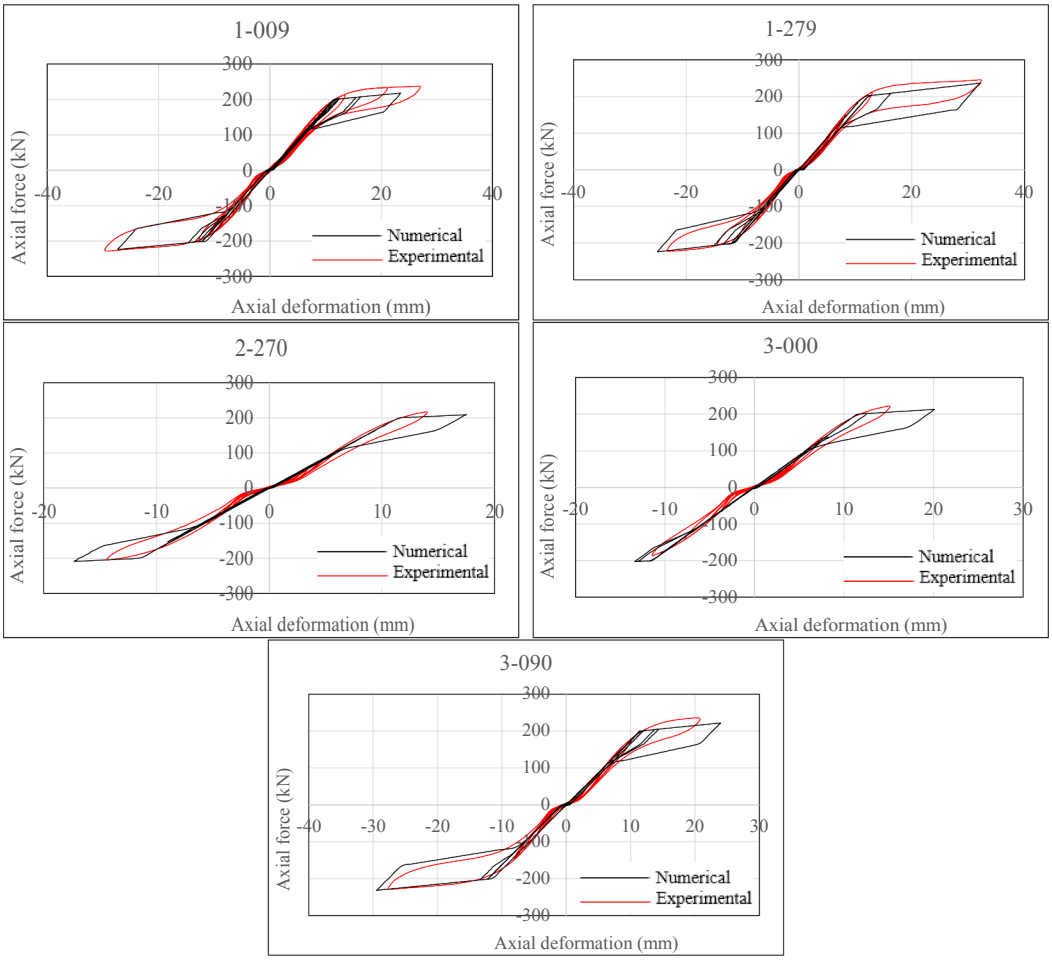

Fig. 17. Experimental and numerical hysteresis response for the 5 records using the closed-loop dynamic testing after model refinement.

Table 2
PBSC model parameters before and after refinement.

Parameter	Before	After
Yield Force, F_y	203.57 kN	200 kN
Initial Stiffness, k_1	31,808 kN/m	17,500 kN/m
Post-Yield Stiffness, k_2	906.46 kN/m	1500 kN/m
Reverse Transformation End Force, F_{ft}	259.6 kN	290 kN
Reverse Transformation Start Force, F_{rt}	188.3 kN	165 kN
Unloading Force Turn Factor, α	0.325	0.55
Residual Deformation Factor, ß	0.1	0.04
Sliding Rules	Checked	Checked

and compared again to the original response to fully close the loop and validate the test procedure, which is named as closed-loop dynamic (CLD) testing. The major findings of the study are highlighted as follows:

- The PBSC showed perfect self-centering ability with good energy dissipation. Finite element models were generated, and fast nonlinear analysis was conducted using the same loading protocol. Excellent agreement in the seismic response of the proposed system for the experimental and numerical results was achieved.
- Strain rate effect was investigated where varying loading rates were considered on the same specimen. The maximum force-deformation responses were very close, but the energy dissipation decreased noticeably as the rate increased. The maximum reduction observed for the X50 rate with around 60% less energy dissipation.
- The proposed closed-loop dynamic (CLD) testing technique was adopted and conducted on the frame building equipped with the PBSC system. The dynamic deformation response was obtained, scaled down, and applied to the fabricated specimen. The new closed-loop dynamic testing technique proved to be reliable where a reasonable agreement was obtained between the dynamic simulation and the experimental results. This proposed method minimizes the time and computational efforts required compared to the shake table and hybrid simulation testing method.
- The proposed CLD test methodology possesses the advantage of hybrid simulation in terms of accurate integrated experimental testing of a real specimen with a refined numerical model and the advantage of quasi-static and dynamic testing in terms of reduced time and effort needed for the investigation.
- Dynamic testing of the proposed system, through closed-loop dynamic testing method, highlighted the need to adjust the modeling parameters which were initially developed based on pure finite element simulation. The adjusted parameters, based on the dynamic testing results, improved to a great extent the ability of the numerical model to capture the actual response of the system.
- In systems where strain rate effect is highly noticeable and observed, the closed-loop dynamic testing may not provide a similar validation like the one presented herein. Further experimental investigation can be adopted on different systems to generalize the concept. Nevertheless, for systems with behavior similar to PBSC, this technique can be an affordable option to validate the design process and the feasibility of adopting new systems.

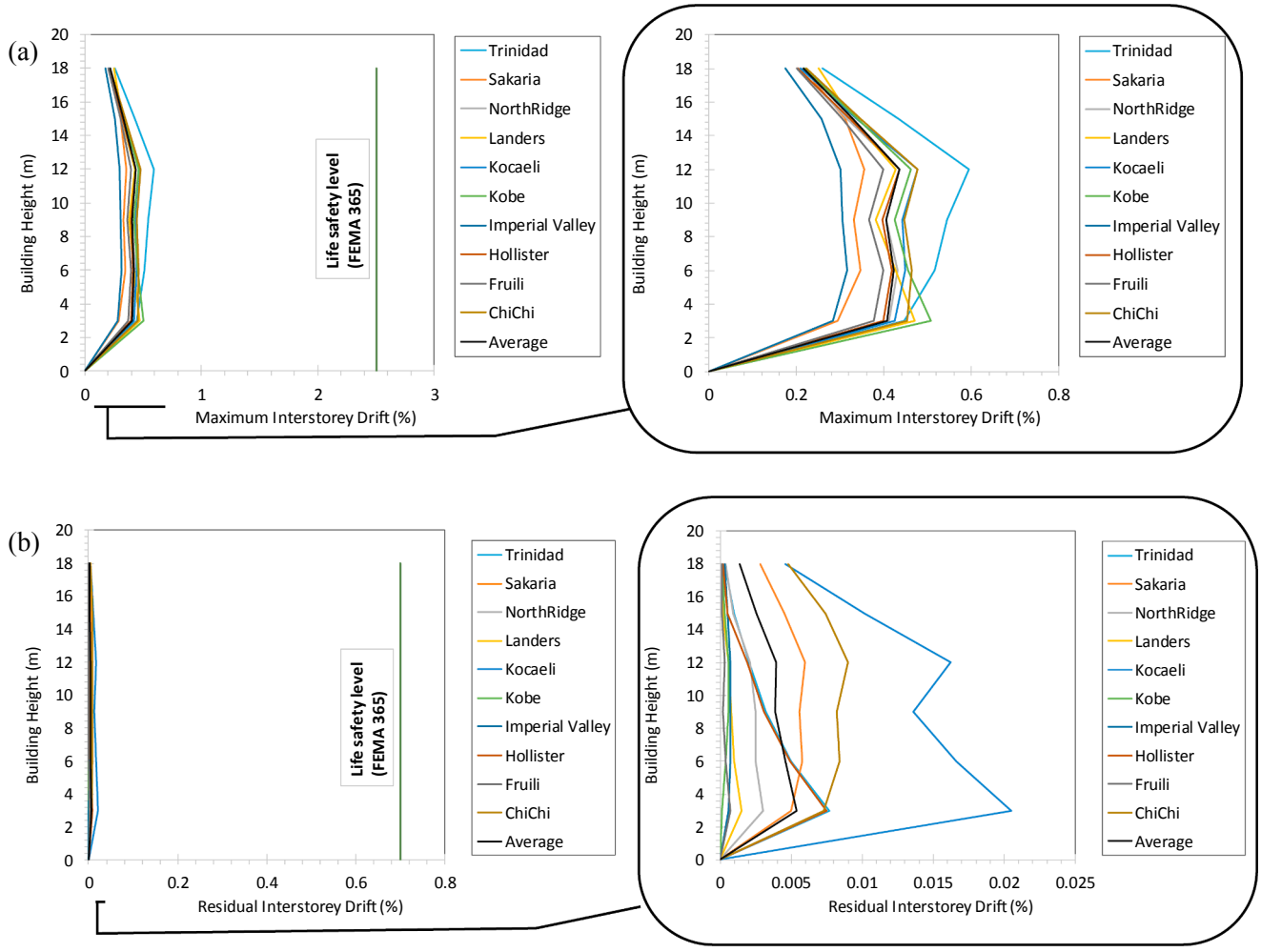

Fig. 18. (a) Maximum Interstory Drift % (b) Residual Interstory Drift %

- The proposed PBSC system overcomes the other available self-centering systems in its simplicity and constructability. Such bracing will not only be an efficient technique for new buildings but also for possible retrofitting of older deficient structures.

Acknowledgements

The financial contribution of Natural Sciences and Engineering Research Council of Canada (NSERC) through Discovery Grant was critical to conduct this study and is gratefully acknowledged.

Appendix A

See Table A.1.

Table A1
Scaling laws for dynamic models.

Physical Quantity	Notation	Model scaling factor
Length	l	l_r
Time	t	$l_r^{1/2}$
Frequency	ω	$l_r^{-1/2}$
Velocity	v	$l_r^{1/2}$
Gravitational acceleration	g	l
Acceleration	a	l
Mass density	ρ	*
Strain	ε	l
Stress	σ	l
Modulus of Elasticity	E	l
Specific Stiffness	E/ρ	—
Displacement	δ	l_r
Force	F	l_r^2

*For lumped masses: $Mr = E_r l_r$.

Appendix B. Supplementary material

Supplementary data to this article can be found online at https://doi.org/10.1016/j.engstruct.2019.05.103.

References

[1] Abdulridha A, Palermo D, Foo S, Vecchio FJ. Behavior and modeling of superelastic shape memory alloy reinforced concrete beams. Eng Struct 2013;49:893–904.
[2] Choi E, Youn H, Park K, Jeon J-S. Vibration tests of precompressed rubber springs and a flag-shaped smart damper. Eng Struct 2017;132:372–82.
[3] Christopoulos C, Tremblay R, Kim H-J, Lacerte M. Self-centering energy dissipative bracing system for the seismic resistance of structures: development and validation. J Struct Eng 2008;134(1):96–107.
[4] CSA. Design of steel structures. CSA Standard S16-09. Rexdale, Ont.: Canadian Standards Association; 2009.
[5] CSA. Design of steel structures. CSA Standard S16-14. Rexdale, Ont.: Canadian Standards Association; 2014.
[6] Cortés-Puentes WL, Palermo D. SMA tension brace for retrofitting concrete shear walls. Eng Struct 2017;140:177–88.
[7] DesRoches R, McCormick J, Delemont M. Cyclic properties of superelastic shape memory alloy wires and bars. J Struct Eng 2004;130(1):38–46.
[8] Dolce M, Cardone D. Mechanical behaviour of shape memory alloys for seismic applications 2. Austenite NiTi wires subjected to tension. Int J Mech Sci 2001;43(11):2657–77.
[9] Dolce M, Cardone D, Marnetto R. Implementation and testing of passive control devices based on shape memory alloys. Earthquake Eng Struct Dyn 2000;29(7):945–68.
[10] Elnashai AS, Gencturk B, Kwon O-S, Al-Qadi IL, Hashash Y, Roesler JR, et al. The Maule (Chile) earthquake of February 27, 2010: Consequence assessment and case studies; 2010.
[11] Elwood KJ. Performance of concrete buildings in the 22 February 2011 Christchurch earthquake and implications for Canadian codes. Can J Civ Eng 2013;40(3):759–76.
[12] Haque A. Seismic performance evaluation and design of a novel piston based self-centering bracing system. University of British Columbia; 2017.
[13] Haque AR, Alam MS, Piston based self-centering brace apparatus. US Patent, 9,683, 365; 2017.
[14] Haque AR, Alam MS. Hysteretic behaviour of a piston based self-centering (PBSC) bracing system made of superelastic SMA bars–a feasibility study. Structures 2017;12:102–14.
[15] IBC. Study of impact and the insurance and economic cost of a major earthquake in British Columbia and Ontario/Québec. Boston, MA, 2013. p. 345.
[16] Issa AS, Alam MS. Seismic performance of a novel single and double spring-based piston bracing. J Struct Eng 2018;145(2):04018261.
[17] Kammula V, Erochko J, Kwon OS, Christopoulos C. Application of hybrid-simulation to fragility assessment of the telescoping self-centering energy dissipative bracing system. Earthquake Eng Struct Dyn 2014;43(6):811–30.
[18] Krawinkler H. Scale effects in static and dynamic model testing of structures; 1988.
[19] Lexcellent C, Bourbon G. Thermodynamical model of cyclic behaviour of Ti-Ni and Cu-Zn-Al shape memory alloys under isothermal undulated tensile tests. Mech Mater 1996;24(1):59–73.
[20] McCrum D, Williams M. An overview of seismic hybrid testing of engineering structures. Eng Struct 2016;118:240–61.
[21] Moncarz PD, Krawinkler H. Theory and application of experimental model analysis in earthquake engineering 1981;vol. 50.
[22] Mueller A. Real-time hybrid simulation with online model updating; 2014.
[23] Nakata N, Dyke S, Zhang J, Mosqueda G, Shao X, Mahmoud H, et al. Hybrid simulation primer and dictionary. Network for earthquake engineering simulation, NEES; 2014.
[24] NBCC. National building code of Canada. Ottawa, Ont.: Institute for Research in Construction, National Research Council of Canada; 2010.
[25] Ozbulut OE. Seismic protection of bridge structures using shape memory alloy-based isolation systems against near-field earthquakes. Texas A&M University; 2010.
[26] Ozbulut OE. Neuro-fuzzy model of superelastic shape memory alloys with application to seismic engineering (Doctoral dissertation). Texas A & M University; 2010.
[27] Ozbulut OE, Hurlebaus S, Desroches R. Seismic response control using shape memory alloys: a review. J Intell Mater Syst Struct 2011;22(14):1531–49.
[28] Qiu C-X, Zhu S. Performance-based seismic design of self-centering steel frames with SMA-based braces. Eng Struct 2017;130:67–82.
[29] Qiu C, Zhu S. Shake table test and numerical study of self-centering steel frame with SMA braces. Earthquake Eng Struct Dyn 2016.
[30] Roeder CW, Lumpkin EJ, Lehman DE. Seismic performance assessment of concentrically braced steel frames. Earthquake Spectra 2012;28(2):709–27.
[31] Speicher MS, DesRoches R, Leon RT. Investigation of an articulated quadrilateral bracing system utilizing shape memory alloys. J Constr Steel Res 2017;130:65–78.
[32] Takeuchi T, Nakamura H, Kimura I, Hasegawa H, Saeki E, Watanabe A. Buckling restrained braces and damping steel structures: Google Patents; 2004.
[33] Tremblay R, Archambault MH, Filiatrault A. Seismic response of concentrically braced steel frames made with rectangular hollow bracing members. J Struct Eng 2003;129(12):1626–36.
[34] Tremblay R, Christopoulos C. Self-centering energy dissipative brace apparatus with tensioning elements: Google Patents; 2012.
[35] Williams M, Blakeborough A. Laboratory testing of structures under dynamic loads: an introductory review. Philos Trans Royal Soc Lond A: Math Phys Eng Sci 2001;359(1786):1651–69.
[36] Wu J, Phillips BM. Passive self-centering hysteretic damping brace based on the elastic buckling mode jump mechanism of a capped column. Eng Struct 2017;134:276–88.
[37] Xie Q, Zhou Z, Huang J, Zhu D, Meng S. Finite-element analysis of dual-tube self-centering buckling-restrained braces with composite tendons. J Compos Constr 2016:04016112.
[38] Xu L-H, Fan X-W, Li Z-X. Development and experimental verification of a pre-pressed spring self-centering energy dissipation brace. Eng Struct 2016;127:49–61.
[39] Xu LH, Fan XW, Li ZX. Cyclic behavior and failure mechanism of self-centering energy dissipation braces with pre-pressed combination disc springs. Earthquake Eng Struct Dyn 2016.
[40] Zhang C, Xu H, Li H, Ou J. Dynamic testing of structural active control system based on a hybrid test-simulation method. Paper presented at the proc Australian earthquake engineering society conference. 2011.
[41] Zhu S, Zhang Y. Seismic behaviour of self-centring braced frame buildings with reusable hysteretic damping brace. Earthquake Eng Struct Dyn 2007;36(10):1329–46.